Annexin A5 regulates surface αvβ5 integrin for retinal clearance phagocytosis

Chen Yu[1], Luis E. Muñoz[2], Mallika Mallavarapu[1], Martin Herrmann[2], and Silvia C. Finnemann[1*]

[1]Department of Biological Sciences, Center for Cancer, Genetic Disease, and Gene Regulation, Fordham University, Bronx, NY, USA. [2]Friedrich-Alexander-University Erlangen-Nürnberg (FAU), Department of Internal Medicine 3 – Rheumatology and Immunology, Universitätsklinikum Erlangen, Erlangen, Germany.

*Author for correspondence:
Silvia C. Finnemann, Ph.D.
Fordham University
441 East Fordham Road
Bronx, NY10458
Phone 718-817-3630
Fax: 718-817-3514
E-mail: finnemann@fordham.edu

JCS Advance Online Article. Posted on 12 September 2019

Summary statement:

Cytosolic annexin A5 regulates the particle binding step of clearance phagocytosis by increasing levels of apical surface αvβ5 integrin receptors of retinal pigment epithelial cells.

Abstract

Diurnal clearance phagocytosis by the retinal pigment epithelium (RPE) is a conserved efferocytosis process whose binding step is mediated by αvβ5 integrin receptors. Two related annexins A5 (ANXA5) and A6 (ANXA6) share an αvβ5 integrin-binding motif. Here, we report that ANXA5 but not ANXA6 regulates the binding capacity for spent photoreceptor outer segment fragments or apoptotic cells by fibroblasts and RPE. ANXA5$^{-/-}$ RPE *in vivo* like αvβ5-deficient RPE lacks the diurnal burst of phagocytosis that follows photoreceptor shedding in wild-type retina. Increasing ANXA5 in cells lacking αvβ5 or increasing αvβ5 in cells lacking ANXA5 does not affect particle binding. Association of cytosolic ANXA5 and αvβ5 integrin in RPE in culture and *in vivo* further supports their functional interdependence. Silencing ANXA5 is sufficient to reduce levels of αvβ5 receptors at the apical, phagocytic surface of RPE cells. The effect of ANXA5 on surface αvβ5 and on particle binding requires the C-terminal ANXA5 annexin repeat but not its unique N-terminus. These results identify a novel role for ANXA5 specifically in the recognition/binding step of clearance phagocytosis that is essential to retinal physiology.

Introduction

In the mammalian retina, continuous renewal of the light-sensitive outer segment portions of photoreceptor neurons involves shedding of spent photoreceptor outer segment fragments (POS) and their prompt clearance from the retina through phagocytosis by the retinal pigment epithelium (RPE) (Young, 1967; Young and Bok, 1969). POS turnover is regulated by light and circadian rhythms such that rods (which constitute the vast majority of photoreceptors in both rodent and human retina) shed POS in the morning upon light onset, which is followed by a burst of phagocytosis by RPE cells (LaVail, 1976). Life-long photoreceptor outer segment renewal is essential for vision.

RPE cells employ a molecular machinery for POS phagocytosis that is conserved evolutionarily and shared with other cell types (Kloditz et al., 2017). These forms of clearance phagocytosis for swift and non-inflammatory removal of apoptotic cells and debris, also known as efferocytosis, are triggered by particle externalization of the anionic membrane lipid phosphatidylserine (PS), which serves as “eat me” signal (Segawa and Nagata, 2015).

Particle binding and engulfment are two independent steps of clearance phagocytosis that are both saturable and dependent on specific and distinct phagocyte surface receptors. Phagocytic cells may employ numerous cell surface receptors to recognize and bind PS-positive phagocytic particles often via soluble bridge proteins. Receptor usage depends on both particle and phagocytic cell type and includes αvβ3 and αvβ5 integrins as receptors that mediate particle binding but do not directly promote engulfment (Finnemann and Rodriguez-Boulan, 1999; Savill et al., 1990). In the mammalian retina, the integrin ligand milk fat globule-EGF factor 8 (MFG-E8) bridges PS on POS with apical αvβ5 integrin receptors of the RPE (Finnemann, 2003; Nandrot et al., 2004; Nandrot et al., 2007). Recognition of POS by αvβ5 integrin binding receptors via focal adhesion kinase stimulates the engulfment receptor Mer tyrosine kinase (MerTK) whose activation is required for particle internalization (Feng et al., 2002; Finnemann, 2003). Mice lacking αvβ5 integrin lose the synchronized diurnal burst of RPE phagocytosis and develop age-related blindness (Nandrot et al. 2004).

Annexins comprise a sizeable family of proteins with conserved annexin repeats mediating protein-lipid and protein-protein interactions in many physiological processes (Gerke et al., 2005). Proteomic studies have found annexins A2, A4, A5 and A6 in human

RPE cells (West et al., 2003) and annexins A2 and A5 in apical microvilli of mouse RPE (Bonilha et al., 2004). Annexin A2 contributes to POS phagocytosis likely by affecting phagosome F-actin recruitment or trafficking (Law et al., 2009). Specific functions of other annexins in the RPE have yet to be elucidated.

Our studies presented here were prompted by reports of a β5 integrin binding domain in annexin A5 (from hereon: ANXA5) with hitherto unknown physiological function (Andersen et al., 2002; Cardo-Vila et al., 2003). Exploring if and how ANXA5 contributes to αvβ5 integrin-dependent clearance phagocytosis we show here that ANXA5 regulates RPE phagocytic activity in both cell culture and *in vivo.* ANXA5 employs C-terminal motifs to associate with αvβ5 receptors causing an increase in receptor levels at the apical, phagocytic surface of the RPE. These findings reveal a novel and essential function of intracellular ANXA5 in clearance phagocytosis.

Results

Annexin A5 but not annexin A6 promotes clearance phagocytosis of either POS or apoptotic cells by mouse embryonic fibroblasts

ANXA5 has been shown to be able to bind to the intracellular domain of integrin β5 via the peptide motif SnYSMnnnD (Cardo-Vila et al., 2003). The alignment in figure 1A shows that this motif is also present in annexin A6 (ANXA6) but not in other human annexins, and this motif is conserved in mouse ANXA5 and ANXA6 (Fig. S1). With both ANXA5 and ANXA6 expressed by RPE cells we asked if either annexin might be relevant to their αvβ5 integrin dependent POS uptake pathway. We previously found that mouse embryonic fibroblasts (MEFs) like RPE cells avidly bind and engulf POS in experimental phagocytosis assays using a phagocytic mechanism via αvβ5 integrin, FAK, and MerTK (Nandrot et al., 2012). Thus, we established immortalized lines of ANXA5$^{-/-}$ and ANXA6$^{-/-}$ MEFs to test their phagocytic function in response to challenge with purified POS. We manipulated expression levels of ANXA5 using recombinant adenovirus by re-expressing mouse ANXA5 in ANXA5$^{-/-}$ MEFs and by overexpressing mouse ANXA5 in ANXA6$^{-/-}$ MEFs followed by POS challenge at 20^{o}C, a restrictive temperature at which cells can bind POS via αvβ5 integrin but cannot engulf POS (Finnemann and Rodriguez-Boulan, 1999). We used infection conditions to yield ANXA5 levels in ANXA5$^{-/-}$ MEFs that were similar to endogenous levels of ANXA6$^{-/-}$ MEFs

and total ANXA5 levels in ANXA6$^{-/-}$ that were increased only moderately, by 2.2-fold on average (Fig. 1B,C). As control we expressed β-gal (β-gal) in either cell line also via adenovirus (Fig. 1B,C). Quantification by immunoblotting for the POS marker protein opsin revealed that ANXA5$^{-/-}$ MEFs expressing β-gal bound 40% less POS material than ANXA6$^{-/-}$ MEFs expressing β-gal (Fig. 1B,D). Expressing ANXA5 was sufficient to restore POS binding by ANXA5$^{-/-}$ MEFs and to significantly increase POS binding by ANXA6$^{-/-}$ MEFs (Fig. 1B,D). In these experiments we directly compared ANXA5$^{-/-}$ MEFs and ANXA6$^{-/-}$ MEFs as these two immortalized lines derived from mouse strains of the same genetic background and with similar genetic manipulations. To test if wild-type MEFs also responded to overexpression of mouse ANXA5 we additionally quantified POS binding by wild-type MEFs infected with β-gal or ANXA5 adenovirus as before. Supplementary Figure S2 shows increased POS binding by wild-type MEFs overexpressing ANXA5 indicating a role of ANXA5 in particle binding common to MEF lines. To test whether manipulating ANXA6 also alters POS binding, we transfected ANXA6$^{-/-}$ MEFs with expression plasmids encoding mouse ANXA6 or GFP as transfection control. POS challenge at 20^{o}C followed by cell harvest and immunoblotting showed that ANXA6$^{-/-}$ MEFs expressed exogenous ANXA6 or GFP proteins (Fig. 1E) but did not differ in POS binding (Fig. 1E,F).

Next, we examined whether manipulating ANXA5 levels in MEFs might also affect clearance of apoptotic cells. We used UV irradiation to induce apoptosis of CEM cells, a T-cell line. We then used these apoptotic cells to challenge ANXA5$^{-/-}$ MEFs that expressed either β-gal or ANXA5 at 20^{o}C to promote apoptotic cell binding or at 37^{o}C to promote engulfment. Immunoblotting for the T-cell marker zap-70 showed that ANXA5 re-expression was sufficient to increase binding but not internalization of apoptotic CEM cells by ANXA5$^{-/-}$ MEFs (Fig. 1G-I). Failure of ANXA5$^{-/-}$ MEFs re-expressing ANXA5 to engulf more apoptotic cells suggests that activities of the engulfment machinery are limiting engulfment under the conditions of the assay even if levels of surface-bound apoptotic cells are elevated. Altogether, these findings show that ANXA5 specifically promotes the binding step of efferocytosis of POS or apoptotic cells by MEFs.

Lack of annexin A5 but not annexin A6 abolishes the synchronized diurnal burst of photoreceptor outer segment phagocytosis by the RPE in vivo

To determine whether the findings in MEFs were of physiological relevance to the outer renewal mechanism, we next asked if lack of ANXA5 affects retinal morphology and diurnal RPE clearance phagocytosis *in vivo*. We detected ANXA5 in both neural retina and eyecup tissue of both mouse and rat eyes (Fig. 2A). Consistent with this and with published proteomics data (Bonilha et al., 2004), confocal microscopy showed ANXA5 in wild-type mouse eyes in neural retina, choroid and the RPE including at its apical, surface where the RPE contacts photoreceptor outer segments (Fig. 2B). Lack of ANXA5 antibody immunolabeling in ANXA5$^{-/-}$ tissue confirmed labeling specificity (Fig. 2B). To investigate whether lack of ANXA5 has an impact on diurnal RPE phagocytosis *in vivo*, we counted POS phagosomes in RPE tissue obtained from age- and strain-matched adult WT, ANXA6$^{-/-}$ and ANXA5$^{-/-}$ mice sacrificed at specific times in relation to light onset. Figure 2C shows that WT and ANXA6$^{-/-}$ RPE had higher POS phagosome load than ANXA5$^{-/-}$ RPE at 1.5 hours after light onset, a time of peak phagosome content using this assay. Quantification of POS phagosome content at multiple time points between 0.5 hours and 12 hours after light onset further revealed that the characteristic diurnal variation in POS phagosome load with elevated levels early after light onset is lacking in ANXA5$^{-/-}$ tissue (Fig. 2D, 0.5 and 1.5 hours, compare white and black bars). Instead, POS phagosome content of ANXA5$^{-/-}$ RPE was similar at all time points examined (Fig. 2D, compare black bars). This resulted in an elevated ANXA5$^{-/-}$ RPE POS phagosome load at late time points at which WT RPE phagosome load is minimal (Fig. 2D, 9 and 12 hours, compare white and black bars). In contrast, ANXA6$^{-/-}$ RPE phagosome content did not differ from phagosome content of WT RPE at any of the time points tested (Fig. 2D, compare white and gray bars). Taken together, these results demonstrate that ANXA5 is required for the diurnal burst of clearance phagocytosis by the RPE *in vivo.*

Annexin A5 is required for POS binding but not subsequent F-actin phagocytic cup formation or internalization by RPE cells

To evaluate the role of ANXA5 in the phagocytosis process specifically of RPE cells, we next quantified POS phagocytosis by unpassaged primary RPE cells manipulated to express more or less ANXA5. Transient transfection of RPE cells with ANXA5 small interfering RNAs (siRNAs) or control non-targeting siRNAs did not visibly alter cell morphology (Fig. 3A). However, following POS challenge we observed fewer bound POS on RPE treated with ANXA5 siRNA than on control RPE (Fig. 3B). Quantification by immunoblotting revealed that reduction of ANXA5 protein levels by 79% caused a 49% reduction in POS binding (Fig. 3C-E). Silencing of ANXA5 was specific as it had no effect on levels of annexin A2 (Fig. 3C). Next, we applied recombinant adenoviruses to transiently overexpress either ANXA5 or β-gal in RPE cells. 3.6-fold higher total ANXA5 protein levels (Fig. 3F,G) compared to control cells expressing β-gal increased POS binding by 50% (Fig. 3F,H). These results demonstrate that like in MEFs, decreasing or increasing ANXA5 in RPE cells is sufficient to suppress or promote POS binding, respectively.

ANXA5 has been proposed to regulate F-actin cytoskeletal assembly in blood clotting (Tzima et al., 2000). Bound POS trigger formation in RPE cells of an F-actin-based structure called phagocytic cup followed by further F-actin dynamics during particle engulfment (Mao and Finnemann, 2012; Bulloj et al., 2013). Thus, we set out to test if ANXA5 silencing alters POS phagocytic cup formation or engulfment by RPE cells. In these experiments, we wished to exclude secondary effects on phagocytic cups and engulfment that could be caused by the unequal numbers of POS bound to ANXA5 silenced versus control cells due to the direct effect of ANXA5 silencing on POS binding. To this end, we limited POS binding by halving the concentration of POS used to challenge the cells. This resulted in equal numbers of POS bound by RPE cells regardless of ANXA5 expression levels (Fig. 4A). To synchronize the different steps of the phagocytic process we used a discontinuous phagocytosis assay challenging RPE cells with fluorescent POS at 20°C to allow binding only, before removing unbound POS and incubating further at 37°C to promote subsequent steps of phagocytosis (Mazzoni et al., 2019). Fixation of cells after 10 min incubation at 37°C followed by F-actin and POS imaging showed normal phagocytic cup recruitment in RPE cells with decreased levels of ANXA5 that was indistinguishable from control cells (Fig. 4A-C). Fixation of cells

after 90 min incubation at 37°C revealed similar POS engulfment by RPE cells regardless of ANXA5 protein levels (Fig. 4D-F). Taken together, these synchronized phagocytosis experiments show that ANXA5 does not directly contribute to phagocytic cup formation or POS internalization by RPE cells.

Annexin A5 is irrelevant to POS binding in the absence of αvβ5 integrin

To investigate the functional relationship of ANXA5 and the primary POS binding receptor of the RPE αvβ5 integrin, we next examined the effect of manipulating ANXA5 on POS binding by β5 integrin$^{-/-}$ (β5$^{-/-}$) mouse primary RPE cells. Overexpressing ANXA5 3.7-fold did not significantly affect POS binding by β5$^{-/-}$ primary RPE (Fig. 5A-C). In contrast and as expected, ANXA5 overexpression by 2.7-fold on average significantly increased POS binding by primary RPE cells lacking MerTK, which bind POS via αvβ5 integrin although they cannot internalize bound POS (Fig. 5D-F) (Nandrot et al., 2012). Of note, we found the same level of endogenous ANXA5 protein in RPE/choroid tissues from WT, β5$^{-/-}$ and MerTK$^{-/-}$ mice indicating that there are no secondary changes in ANXA5 upon elimination of either phagocytic receptor (Fig. S3).

Given the very limited availability of primary mouse RPE and at best partial reduction of ANXA5 obtained through silencing in these cells, we used β5$^{-/-}$ MEFs to expand on these experiments. Manipulating ANXA5 levels in β5$^{-/-}$ MEFs, we roughly halved ANXA5 protein levels by silencing or doubled ANXA5 protein levels by overexpression, respectively (Fig. 6A-B,D-E). Consistent with the data from β5$^{-/-}$ primary RPE, we found that these changes in ANXA5 protein levels had no effect on POS binding by β5$^{-/-}$ MEFs (Fig. 6A-D,F). We previously found that adenovirus-mediated β5-GFP expression increases levels of surface αvβ5-GFP receptors and in turn POS binding by RPE and fibroblasts (Nandrot et al. 2012). Here, we used the same β5-GFP adenovirus to infect ANXA5$^{-/-}$ MEFs. Strikingly, αvβ5-GFP expression did not affect POS binding by ANXA5$^{-/-}$ MEFs (Fig. 6G-I). This was not due to lack of formation of αvβ5-GFP receptors at the cell surface as shown by live surface receptor labeling with αvβ5 receptor antibody that does not recognize mouse αvβ5 (Fig. 6J). Altogether, our experiments manipulating ANXA5 and β5 integrin in cells lacking one or the other demonstrate that the role of ANXA5 in POS binding requires αvβ5 integrin. To determine if ANXA5$^{-/-}$ MEFs retain any integrin-dependent POS binding activity, we next

directly compared POS binding activity of WT, ANXA5$^{-/-}$, and β5$^{-/-}$ MEFs. We found that WT MEFs bind significantly more POS than ANXA5$^{-/-}$ MEFs, and that β5$^{-/-}$ MEFs bind significantly fewer POS than both ANXA5$^{-/-}$ and WT MEFs (Fig. 6K,L, compare gray bars). Moreover, adding cilengitide, a cyclic RGD peptide specifically inhibiting αv-containing integrins (Lode et al., 1999) robustly reduced POS binding by WT and by ANXA5$^{-/-}$ MEFs but had no effect on β5$^{-/-}$ MEFs (Fig. 6K,L, compare gray and white bars for each cell type). These data confirm POS binding defects of both ANXA5$^{-/-}$ and β5$^{-/-}$ MEFs. They further indicate that ANXA5$^{-/-}$ but not β5$^{-/-}$ MEFs retain a reduced level of αv-integrin dependent POS binding activity.

Annexin A5 associates with αvβ5 integrin and promotes its surface localization

To investigate whether ANXA5 may associate with αvβ5 integrin in the RPE, we first labeled apical αvβ5 receptor dimers in live, chilled primary rat RPE followed by fixation, permeabilization and co-staining with ANXA5 antibody. Figure 7A shows select individual confocal microscopy x-z planes representing the very top of the apical surface, the main location of αvβ5 labeling, and a plane 0.13 µm below the apical surface, with abundant ANXA5. The x-z scan also shown confirms that both αvβ5 and ANXA5 labels are apical with the αvβ5 signal detected just above the ANXA5 signal. The αvβ5 receptor labeling antibody and the secondary antibodies extend into the apical extracellular space whereas ANXA5 is cytosolic. We thus interpret the image as showing apical membrane αvβ5 receptors with sub-apical membrane ANXA5. As complementary approach, we performed immunoprecipitations (IPs) and found that ANXA5 antibody specifically co-isolates β5 integrin from lysates of either primary RPE cells (Fig. 7B) or of eyecup tissues (dissected rat eyes containing the RPE and choroid tissue, but not neural retina, cornea or lens) (Fig. 7C). We did not detect this complex if we performed the co-isolation experiment using buffers devoid of Ca^{2+} suggesting that the association of ANXA5 with the β5 integrin cytosolic tail is Ca^{2+}-dependent (Fig. 7D). Together, these data imply that cytosolic ANXA5 resides in an apical complex with αvβ5 integrin in the RPE.

We followed up on these association studies to probe the mechanism through which silencing ANXA5 affected αvβ5 integrin in RPE cells. Whole lysate immunoblotting did not show differences in αvβ5 receptor subunit levels, and whole lysate αvβ5 receptor IPs did not

show differences in total αvβ5 dimer levels in cells with reduced levels of ANXA5 (Fig. 7D, panels lysate and total IP, 7E). However, selective IP of apical surface αvβ5 showed a significant decrease by 60% on average in apical surface αvβ5 heterodimers in cells with reduced ANXA5 as compared to control cells (Fig. 7D, panel surface IP, 7E). It should be noted that due to differences in experimental procedures, we cannot be sure that total αvβ5 IPs and αvβ5 surface IPs are directly comparable. To avoid overinterpretation, each type of IP was therefore quantified separately. Complementary surface receptor immunolabeling followed by confocal microscopy, although only semi-quantitative, confirmed this result (Fig. 7F). Altogether, our results show that ANXA5 resides in a surface complex with αvβ5 and promotes localization of this essential particle binding receptor at the apical, phagocytic surface of RPE cells.

The C-terminal annexin repeat 4 is required for activity of annexin A5 in αvβ5 integrin regulation and POS binding, but the annexin A5-unique N-terminus is dispensable

Finally, to probe the physical and functional interaction between ANXA5 and αvβ5 integrin, we generated four expression constructs encoding DDK-myc tagged mouse full-length or truncated ANXA5: full-length ANXA5 (FL), A5-nd20 (lacking the N-terminal 20 amino acids, which are unique to ANXA5), A5-cd67 (lacking the C-terminal 67 amino acids comprising the entire annexin repeat 4), and A5-cd20 (lacking the C-terminal 20 acids containing the reported integrin β5 binding motif in annexin repeat 4) (Fig. 8A). Whole cell lysate immunoblotting of RPE cells infected with adenoviruses encoding β-gal or these ANXA5 constructs showed that all forms of ANXA5 were expressed at the expected molecular weight and at roughly equal levels (Fig. 8B). αvβ5 receptor subunit levels were unaffected by ANXA5 overexpression (Fig. 8B).

We next tested which forms of exogenous ANXA5 formed a complex with endogenous αvβ5 receptors in RPE cells. Surface IPs of αvβ5 integrin detected FL ANXA5 and A5-nd20 as coprecipitate, but not A5-cd67 (Fig. 8C). Unexpectedly, A5-cd20 lacking the reported β5 integrin binding motif consistently coprecipitated with surface αvβ5, albeit at low levels (Fig. 8C). However, comparison of surface αvβ5 receptor levels in these IPs showed that overexpression of FL ANXA5 or A5-nd20 significantly increased αvβ5 surface receptor levels, compared with RPE cells expressing β-gal, while overexpression of A5-cd67 or A5-

cd20 had no effect (Fig. 8D-F). We conclude that A5-cd20 by itself cannot interact with αvβ5 receptors and thus does not increase levels of αvβ5 at the cell surface. Yet, A5-cd20 co-isolates with surface αvβ5 complexes. While the mechanism of complex assembly needs further investigation, we speculate that A5-cd20 may retain phosphatidylserine binding activity as it contains part of annexin repeat 4 (Wang et al., 2017). Alternatively, A5-cd20 may assemble with endogenous intact ANXA5 in ANXA5/A5-cd20 trimers (Oling et al., 2000). However, only overexpression of A5-FL or A5-nd20 was sufficient to significantly increase POS binding by RPE cells while overexpression of A5-cd67 or A5-cd20 had no effect on POS binding, which was the same as POS binding by control cells expressing β-gal (Fig. 8G,H).

Collectively, these results show that eliminating either the entire annexin repeat 4 or its stretch with the reported integrin β5 binding motif precludes ANXA5 from increasing αvβ5 surface levels and consequently POS binding. In contrast, the N-terminus in which ANXA5 differs from all other annexins is not required for this function.

Discussion

In this study, we identify a novel role for cytosolic ANXA5 in clearance phagocytosis. Our data demonstrate that ANXA5 contributes specifically to phagocytic particle binding by promoting surface localization of αvβ5 integrin, which increases activity of this particle binding receptor.

Our data provide evidence for functional interaction between αvβ5 integrin and ANXA5 *in vivo* and in a specific physiological context. While our experiments cannot distinguish between direct and indirect interactions of ANXA5 and αvβ5, they complement well earlier studies on interactions *in vitro* between ANXA5 and αvβ5 including pulldown experiments demonstrating that the two can interact directly (Andersen et al., 2002; Cardo-Vila et al., 2003).

Our results show that ANXA5 impacts the particle binding step (but not the distinct engulfment step) of clearance phagocytosis of either POS or apoptotic cells by MEFs and by RPE implying a function that is not restricted to a specific phagocytic cell or cell debris particle. Given the enormous importance of clearance phagocytosis for tissue homeostasis and the wide-spread expression of both ANXA5 and αvβ5 integrin this suggests a conserved

physiological contribution for ANXA5 in particle binding in preparation for engulfment and digestion across tissues. However, retinal clearance phagocytosis is unique in that there is no redundancy or compensation for loss of αvβ5 integrin or its ligand MFG-E8 such that loss of either eliminates the diurnal peak of POS clearance (Nandrot et al., 2004; Nandrot et al., 2007). Furthermore, activity of αvβ5 integrin in the RPE is tightly regulated including at the level of lateral interactions with its co-receptor CD81, which also affects αvβ5 localization to the apical, phagocytic surface of these avid phagocytes, which must take up numerous spent POS every day for life in a burst after light onset while maintaining retinal adhesion to intact outer segments at all other times (Chang and Finnemann, 2007). Here, we find that ANXA5$^{-/-}$ mice phenocopy β5$^{-/-}$ and MFG-E8$^{-/-}$ mice with respect to the lack of the daily rhythm of POS clearance. Our cell culture data showing no effect of ANXA5 manipulation in cells lacking αvβ5 further support the dependence of ANXA5 on αvβ5 in the RPE phagocytic mechanism. In contrast, some αvβ5 receptors reside at the cell surface without ANXA5 as seen with surface αvβ5-GFP in ANXA5$^{-/-}$ MEFs. We also found that POS binding activity of ANXA5$^{-/-}$ MEFs is reduced compared to activity of WT MEFs but higher than POS binding activity of β5$^{-/-}$ MEFs, and remains sensitive to αv-integrin inhibition. Thus, ANXA5 augments but is not absolutely required for cells to have surface αvβ5. Altogether, surface levels of αvβ5 receptors are highly regulated, and relative contributions of CD81 and ANXA5 may vary with cell context.

Loss of ANXA5 may have subtle consequences for clearance phagocytosis by other cell types for two reasons. Firstly, ANXA5 links to αvβ5 integrin specifically via defined protein motifs rather than affecting clearance recognition receptors indiscriminately. Yet, cells other than RPE that function in clearance phagocytosis are known to employ a variety of clearance receptors. As example, αvβ3 integrin is rather similar structurally to αvβ5 and the two may have overlapping roles in clearance phagocytosis, but the β3 integrin cytoplasmic tail does not share the β5 integrin domain that can bind to ANXA5 *in vitro* (Andersen et al., 2002). αvβ3 and αvβ5 are co-expressed by macrophages in which they compete for apoptotic debris or POS (Finnemann and Rodriguez-Boulan, 1999). While RPE cells also co-express the two integrins, αvβ3 receptors localize basally and thus are not available to the apical phagocytic machinery of the RPE (Finnemann et al., 1997).

Secondly, understanding roles of ANXA5 may be complicated by its co-expression in many cell types with other annexin family members especially the highly related ANXA6. ANXA6 is thought to be derived from duplication and fusion of ANXA5 and ANXA10 genes in vertebrate evolution (Gerke and Moss, 2002). Like ANXA5, ANXA6 can bind phosphatidylserine (Gerke et al, 2005). Furthermore, ANXA6 shares the conserved β5 integrin binding domain with ANXA5. Yet, our data do not support a role for ANXA6 in clearance phagocytosis *in vivo* or *in vitro*: peak phagosome content of ANXA6$^{-/-}$ RPE *in situ* is normal; ANXA6$^{-/-}$ MEFs respond to ANXA5 overexpression like wild-type MEFs by increasing POS binding; restoring ANXA6 in ANXA6$^{-/-}$ MEFs has no effect on POS binding (arguing against an inhibitory effect of ANXA6 on ANXA5); and our acute manipulation assays do not suggest compensatory changes in ANXA6 levels. These results are somewhat surprising as our deletion mutant experiments show that the shared β5 integrin binding domain is required for ANXA5 contribution to POS binding while the ANXA5 unique N-terminus is dispensable. These data suggest that either the motif is required but not sufficient for this function by ANXA6, or that it is blocked in ANXA6 but available for interaction with αvβ5 in ANXA5. A third possibility is that ANXA6 fails to interact with αvβ5 integrin in the RPE because it may not be able to distribute to the apical, phagocytic surface of the RPE.

ANXA5 is best known for its binding affinity for phosphatidylserine, the universal “eat me” signal exposed by apoptotic cells and POS (Fadok et al., 2001; Ruggiero et al., 2012). ANXA5 does not have a conventional secretion signal but it is detected extracellularly and for instance localizes to extracellular matrix in bone and cartilage (Pfaffle et al., 1988). Masking externalized phosphatidylserine with excess recombinant ANXA5 added extracellularly is sufficient to inhibit POS binding by RPE cells (Ruggiero et al., 2012). In agreement, lack of extracellular ANXA5 increases capacity by cultured ANXA5$^{-/-}$ macrophages to phagocytose phosphatidylserine-exposing necrotic cells, and immunogenicity of apoptotic and necrotic cells *in vivo* and *in vitro* differs depending on whether dying cells are opsonized by extracellular ANXA5 (Frey et al., 2009; Muñoz et al., 2007). The results presented in this study imply a role for intracellular ANXA5 in RPE cells as regulator of αvβ5 integrin receptors. However, our experiments do not rule out as yet

unrecognized functions of extracellular ANXA5 in the retina. Understanding these will require further studies.

The precise molecular changes mediated by ANXA5 interactions ultimately increasing αvβ5 receptor levels at the apical, phagocytic surface of the RPE remain to be identified. We found reduced surface levels of αvβ5 in live labeling experiments but similar total αvβ5 dimers in RPE cells, in which ANXA5 was acutely decreased by silencing. We conclude that dimerization of αvβ5 is likely independent of ANXA5. The observed steady-state differences in surface αvβ5 receptors could arise from decreased surface delivery or increased receptor internalization, or a combination of both. Earlier cell culture and *in vitro* studies have demonstrated intriguing functional relationships of ANXA5 and αvβ5 with members of the protein kinase C family including that ANXA5 binding may interfere with PKC function (Schlaepfer et al., 1992; Dubois et al., 1998; Liliental and Chang, 1998; Kheifets et al., 2006). We previously found that pharmacological agents reducing PKC activity increase cytoskeletal anchorage of αvβ5 in RPE cells in turn affecting its capacity to bind POS (Finnemann and Rodriguez-Boulan, 1999). Future studies will test whether activities of ANXA5 in RPE cells relevant to αvβ5 integrin and its POS binding activity require or are upstream of protein kinase C signaling pathways.

Materials and Methods

Reagents were from Millipore-Sigma (St. Louis, MO) or Thermofisher (Waltham, MA) unless otherwise indicated.

Antibodies

Primary antibodies to the following proteins were used: rhodopsin clone B6-30, a kind gift from Paul Hargrave, University of Florida, Gainesville, FL (Adamus et al.,1991); ANXA5 from Hyphen Biomed (Neuville-sur-Oise, France); β-galactosidase, α-tubulin from Abcam (Cambridge, MA); ANXA2, αv integrin, β-actin from BD Transduction Laboratories (San Jose, CA), β-catenin from Millipore-Sigma; ANXA6, β5 integrin, GFP from Santa Cruz (Santa Cruz, CA); αvβ5 integrin dimer antibody P1F6 from Biolegend (San Diego, CA); DDK-tag from Origene (Rockville, MD); RPE65 from Genetex (Irvine, CA); zap70 from Cell Signaling

(Cambridge, MA). Catalog numbers and dilutions of primary antibodies are listed in Supplementary Table 1. Secondary antibodies conjugated with horseradish peroxidase or AlexaFluor dyes were purchased from Jackson ImmunoResearch (West Grove, PA) and Thermofisher, respectively.

Animals and Tissue processing

All procedures involving animals were performed according to the ARVO Guide for Use of Animals in Vision research and *Guide for the Care and Use of Laboratory Animals* (NIH, 8th edition) and approved by the Institutional Animal Care and Use Committee of Fordham University or University of Erlangen, as appropriate. Animals were housed in a 12-h light/12-h dark light cycle with food and water *ad libitum*. Sprague Dawley WT rats, RCS-rdy/rdy-p rats (MerTK$^{-/-}$), β5$^{-/-}$ mice (Huang et al., 2000) and corresponding WT mice all in the same 129T2/SvEmsJ genetic background were housed and bred at the animal facility of Fordham University. ANXA5$^{-/-}$ mice (Brachvogel et al., 2003), ANXA6$^{-/-}$ mice, and WT mice all in the same C57BL/6 genetic background were housed and bred at University of Erlangen, Germany. Mice used tested negative for the rd8 mutation (Chang et al., 2013). Animals used were mixed-gender and 4-11 days of age for primary RPE isolation or 3-8 months of age for other work.

For all procedures, animals were euthanized by CO_2 asphyxiation immediately before tissue harvest. Eye tissues were chilled, dissected and tissue fractions flash-frozen for immunoblotting, fixed in 4% paraformaldehyde (PFA) in PBS for 30 min before embedding in TissueTek for cryosectioning, or fixed in Davidson's fixative (33% ethanol, 22% formaldehyde,11.5% acetic acid) overnight before embedding in paraffin.

RPE and MEF cell culture

Primary RPE cells were isolated from 7-11 day-old rats or 4-6 day-old mice as described previously (Mao and Finnemann, 2012). Briefly, cornea, lens, and vitreous body were removed from freshly enucleated eyes. Rat eyecups were incubated in 1 mg/ml hyaluronidase in Ca^{2+} and Mg^{2+} free Hank's balanced saline solution (HBSS) for 50 min at 37°C. After dissection of iris and neural retina, eyecups were incubated in 2 mg/ml trypsin in HBSS with Ca^{2+} and Mg^{2+} for 50 min (rat) or 33 min (mouse) at 37°C. RPE sheets were

manually collected, re-trypsinized for 1 min and cultured in DMEM with 10% FBS for 4-5 days before experiments. WT, ANXA5$^{-/-}$, ANXA6$^{-/-}$, and β5$^{-/-}$ MEFs were isolated from ~13-day old mouse embryos according to published protocols (Robertson, 1987). In brief, following removal of head and obvious internal organs tissue was minced and then trypsinized in 0.25% trypsin for 15 min at 37°C. Single cells isolated through mechanical trituration were grown with routine passaging in DMEM supplemented with 10% FBS. MEFs were immortalized by infection with virions produced by PA317 cells (ATCC, #CRL-9078) and passaged at least 20 times before use. MEFs were tested and determined to be free of mycoplasma contamination. Genotype of MEFs was routinely tested by immunoblotting, see Fig. 6A,K as example. MEFs were seeded at 50% confluence into 96-well plates one day prior to experiments.

Plasmid or small interfering RNA (siRNA) transfection and adenovirus infection

Plasmids encoding mouse ANXA6 with DDK tag and enhanced green fluorescent protein (eGFP) were from Genscript (Piscataway, NJ) and Clontech, respectively. Electroporation was performed to transfect ANXA6$^{-/-}$ MEFs using Amaxa MEF2 nucleofector kit following the manufacturer's instructions (Lonza, Switzerland). To silence ANXA5 in cells, primary RPE 2 days after plating or MEFs 1 day after plating were transfected with siRNA smartpool specifically targeting rat ANXA5 or non-targeting control siRNAs (Dharmacon/Thermofisher) mixed with Lipofectamine 2000 (Thermofisher) for 48 h, and were treated again for 24 to 48 h before experiments.

A complete mouse ANXA5 cDNA clone was purchased from Origene. Mouse ANXA5 cDNA was cloned into a pCMV6-entry vector to yield a C-terminal DDK-myc tag. Primers from Integrated DNA Technologies (Coralville, IA) used to generate different full length and truncated ANXA5 cDNAs flanked by AsiSI and MluI restriction sites are listed in Supplementary Table 2. Recombinant adenoviruses encoding β-galactosidase (Cell Biolabs, San Diego, CA), rat ANXA5 (Vector Labs, CA) or full-length and truncated mouse ANXA5 with C-terminal DDK-myc tag (Welgen Inc, Worcester, MA) were diluted in serum-free DMEM and applied to 1-2 day-old primary RPE cells or MEFs at 50-70% confluence for 2 h. After retrieval of infection solution, cells were further incubated in complete culture medium for 48 h before experiments.

Immunoblotting

Cultured cells and eyecup tissues were solubilized in HNTG buffer (50 mM HEPES, pH 7.0, 150 mM NaCl, 1.5 mM $MgCl_2$, 10% glycerol, 1% Triton X-100) freshly supplemented with 1 mM PMSF and 1% protease inhibitor cocktail before analysis by standard SDS-PAGE, immunoblotting, and enhanced chemiluminescence detection. Lysate representing equal numbers of cells were compared side by side. Band densities were quantified using Image-J software (NIH, Bethesda, MD).

Immunofluorescence labeling and microscopy

Cultured cells were fixed in 4% PFA in PBS for 20 min, quenched with 50 mM NH_4Cl in PBSCM for 15 min, blocked and permeabilized with PBSCM, 1% BSA, 0.5% Triton X-100 and sequentially incubated with primary antibodies and appropriate secondary antibodies. To live label surface αvβ5 integrin, cells were incubated on ice sequentially with αvβ5 integrin receptor primary antibody and secondary antibody before fixation with 1% PFA in PBS for 10 min.

To stain F-actin phagocytic cups, cells were stained with AlexaFluor488 phalloidin. To distinguish bound and internalized POS, cells fed with Texas-Red labeled POS were stained without permeabilization with opsin antibody and secondary antibody. DAPI was used to counterstain nuclei.

To stain ANXA5 in tissue, 12 µm-thick frozen retina sections were labeled. To detect POS phagosomes, opsin staining of paraffin sections and phagosome counting was performed exactly as described previously (Sethna and Finnemann, 2013). Images were acquired using a Leica TSP5 laser scanning confocal microscopy system and recompiled in Photoshop CS3. Unless otherwise indicated, images show maximum projections of image stacks.

Apoptotic cell phagocytosis assay

CEM cells, a human T lymphoblast cell line was obtained from ATCC (#CCL-119) and cultured in DMEM with 10% FBS. After aspirating the medium, CEM cells were resuspended in PBS and UV-irradiated at the intensity of 45 mJ/m^2. After irradiation, new complete

medium was immediately added to the cells, and then cells were incubated at 37ºC overnight. CEM cells were then resuspended in DMEM and were co-incubated with MEF cells at a ratio of 5:1 for 2 h at 20ºC for binding assays or 37ºC for complete phagocytosis assays. The complete phagocytosis assay was terminated by adding ice-cold 2 mM EDTA in PBS for 5 minutes. Cells were washed three times with PBS containing 1 mM $MgCl_2$ and 0.2 mM $CaCl_2$ (PBS-CM) and lysed with HNTG buffer. Phagocytosis of apoptotic cells was quantified by zap70 T cell specific marker immunoblotting.

Synchronized POS phagocytosis assay

Synchronized cell culture phagocytosis assays were performed following published protocols (Mazzoni et al., 2019). POS particles were isolated from fresh porcine eyes (Parinot et al.) and used unlabeled or pre-labeled with 0.01 mg/ml Texas Red-X. To allow only POS binding, cells were challenged with 10 POS particles per cell in DMEM supplemented with recombinant mouse MFG-E8 at 20°C for 1 h. Cells were washed three times with PBS-CM to remove unbound POS before harvest or, to trigger internalization, further incubation in DMEM supplemented with 2 µg/ml purified human protein S (Aniara/Hyphen Biomed) at 37°C. In select POS binding assays, the POS suspension was supplemented with 0.2 µM cilengitide (Sigma) (cyclic RGD pentapeptide [Arg-Gly-Asp-DPhe-(NMeVal)], Lode et al., 1999) directly before addition to cells. All experiments were terminated either by cell lysis or fixation followed by fluorescence staining. Band intensities and particle fluorescence were quantified using ImageJ software.

Immunoprecipitations

All procedures were performed with cells on ice and using pre-chilled solutions. RPE cells or eyecup tissues from rats sacrificed 30 min after light onset were solubilized in IP lysis buffer (50 mM Tris/Cl, pH 7.8, 150 mM NaCl, 2 mM $CaCl_2$, 1 mM $MgCl_2$, 1% IGEPAL, 1% Triton X-100) supplemented with 1 mM PMSF and 1% protease inhibitor cocktail. Precleared lysates were rotated with 1 µg ANXA5 or non-immune rabbit IgG (Cell signaling) for 1 h. After addition of 20 µl protein G-agarose samples were again rotated for 1 h. Beads were washed three times with wash buffer (50 mM Tris/Cl, pH 8.5, 500 mM NaCl, 2 mM $CaCl_2$, 1 mM $MgCl_2$, 0.1% Triton X-100, 1 mg/ml egg albumin) before protein elution in

reducing sample buffer and analysis by SDS-PAGE/immunoblotting. Select samples were processed in IP lysis buffer and wash buffer without $CaCl_2$.

Surface and total αvβ5 integrin dimeric receptors were quantified as described previously (Nandrot et al., 2012). In brief, to collect surface αvβ5 complexes, cells were rinsed with PBS-CM before incubating intact cells with 20 µg/ml αvβ5 dimer antibody or non-immune mouse IgG in HBSS for 45 min. Cells were then rinsed with PBS-CM twice and lysed in HNTG buffer. To collect total integrin αvβ5 complexes, cells were lysed in HNTG buffer, and cleared whole cell lysates were rotated with 1 µg of P1F6 or non-immune mouse IgG for 2 h. Surface or total immune complexes were collected by rotating with 20 µl protein L agarose for 1.5 h. Beads were washed three times with lysis buffer before protein elution in reducing sample buffer and analysis by SDS-PAGE/immunoblotting.

Data analysis

All data were collected from at least three independent experiments. Means and standard deviations were plotted for all graphs, and individual points are shown when sample size was less than five (GraphPad Prisma 7, La Jolla, CA). Normality and homogeneity of variance were assessed using Kolmogorov-Smirnov test and Levene's test, respectively. Data transformation was conducted to fit test assumptions when necessary. Two group comparisons were analyzed using unpaired Student's two-tailed *t*-test. Comparisons of groups of 3 and greater and multiple factor comparisons were analyzed using ANOVA with Tukey's post hoc tests. $P < 0.05$ was considered statistically significant for all experiments.

Acknowledgements

We thank Frances H. Kazal for excellent technical assistance.

Competing interest

The authors declare that no competing interests exist.

Funding

This work was funded by NIH R01-EY026215 from the National Eye Institute and by the German Research Foundation (DFG CRC1181-C03). S.C.F. holds the Kim B. and Stephen E. Bepler Chair in Biology.

References

Adamus, M. H., Zam, Z. S., Arendt, A., Palczewski, K., McDowell, J. H. and Hargrave, P. A. (1991). Anti-rhodopsin monoclonal antibodies of defined specificity: characterization and application. *Vis Res* **31**, 17–31.

Andersen, M. H., Berglund, L., Petersen, T. E. and Rasmussen, J. T. (2002). Annexin-V binds to the intracellular part of the β5 integrin receptor subunit. *Biochem Biophys Res Comm* **292**, 550-7.

Bonilha, V. L., Bhattacharya, S. K., West, K. A., Sun, J., Crabb, J. W., Rayborn, M. E. and Hollyfield, J. G. (2004). Proteomic characterization of isolated retinal pigment epithelium microvilli. *Mol Cell Proteomics* **3**, 1119-27.

Brachvogel, B., Dikschas, J., Moch, H., Welzel, H., von der Mark, K., Hofmann, C. and Poschl, E. (2003). Annexin A5 is not essential for skeletal development. *Mol Cell Biol* **23**, 2907-13.

Bulloj, A., Duan, W. and Finnemann, S. C. (2013). PI 3-kinase independent role for AKT in F-actin regulation during outer segment phagocytosis by RPE cells. *Exp Eye Res*.

Cardo-Vila, M., Arap, W. and Pasqualini, R. (2003). αvβ5 integrin-dependent programmed cell death triggered by a peptide mimic of annexin V. *Mol Cell* **11**, 1151-62.

Chang, B., Hurd, R., Wang, J. and Nishina, P. (2013). Survey of common eye diseases in laboratory mouse strains. *Invest Ophthalmol Vis Sci* **54**, 4974-81.

Chang, Y. and Finnemann, S. C. (2007). Tetraspanin CD81 is required for the αvβ5 integrin-dependent particle-binding step of RPE phagocytosis. *J Cell Sci* **120**, 3053-63.

Dubois, T., Mira, J. P., Feliers, D., Solito, E., Russo-Marie, F. and Oudinet, J. P. (1998). Annexin V inhibits protein kinase C activity via a mechanism of phospholipid sequestration. *Biochem J* **330 (Pt 3)**, 1277-82.

Fadok, V. A., de Cathelineau, A., Daleke, D. L., Henson, P. M. and Bratton, D. L. (2001). Loss of phospholipid asymmetry and surface exposure of phosphatidylserine is required for phagocytosis of apoptotic cells by macrophages and fibroblasts. *J Biol Chem* **276**, 1071-1077.

Feng, W., Yasumura, D., Matthes, M. T., LaVail, M. M. and Vollrath, D. (2002). Mertk triggers uptake of photoreceptor outer segments during phagocytosis by cultured retinal pigment epithelial cells. *J Biol Chem* **277**, 17016-22.

Finnemann, S. C. (2003). Focal adhesion kinase signaling promotes phagocytosis of integrin-bound photoreceptors. *EMBO J* **22**, 4143-4154.

Finnemann, S. C., Bonilha, V. L., Marmorstein, A. D. and Rodriguez-Boulan, E. (1997). Phagocytosis of rod outer segments by retinal pigment epithelial cells requires αvβ5 integrin for binding but not for internalization. *Proc Natl Acad Sci U S A* **94**, 12932-7.

Finnemann, S. C. and Rodriguez-Boulan, E. (1999). Macrophage and retinal pigment epithelium phagocytosis: apoptotic cells and photoreceptors compete for αvβ3 and αvβ5 integrins, and protein kinase C regulates αvβ5 binding and cytoskeletal linkage. *J Exp Med* **190**, 861-74.

Frey, B., Muñoz, L. E., Pausch, F., Sieber, R., Franz, S., Brachvogel, B., Poschl, E., Schneider, H., Rodel, F., Sauer, R. et al. (2009). The immune reaction against allogeneic necrotic cells is reduced in annexin A5 knock out mice whose macrophages display an anti-inflammatory phenotype. *J Cell Mol Med* **13**, 1391-9.

Gerke, V., Creutz, C. E. and Moss, S. E. (2005). Annexins: linking Ca2+ signalling to membrane dynamics. *Nat Rev Mol Cell Biol* **6**, 449-61.

Gerke, V. and Moss, S. E. (2002). Annexins: from structure to function. *Physiol Rev* **82**, 331-71.

Huang, X., Griffiths, M., Wu, J., Farese, R. V., Jr. and Sheppard, D. (2000). Normal development, wound healing, and adenovirus susceptibility in β5-deficient mice. *Mol Cell Biol* **20**, 755-9.

Kheifets, V., Bright, R., Inagaki, K., Schechtman, D. and Mochly-Rosen, D. (2006). Protein kinase C delta (deltaPKC)-annexin V interaction: a required step in deltaPKC translocation and function. *J Biol Chem* **281**, 23218-26.

Kloditz, K., Chen, Y. Z., Xue, D. and Fadeel, B. (2017). Programmed cell clearance: From nematodes to humans. *Biochem Biophys Res Comm* **482**, 491-497.

LaVail, M. M. (1976). Rod outer segment disk shedding in rat retina: relationship to cyclic lighting. *Science* **194**, 1071-4.

Law, A. L., Ling, Q., Hajjar, K. A., Futter, C. E., Greenwood, J., Adamson, P., Wavre-Shapton, S. T., Moss, S. E. and Hayes, M. J. (2009). Annexin A2 regulates phagocytosis of photoreceptor outer segments in the mouse retina. *Mol Biol Cell* **20**, 3896-904.

Liliental, J. and Chang, D. D. (1998). Rack1, a receptor for activated protein kinase C, interacts with integrin beta subunit. *J Biol Chem* **273**, 2379-83.

Lode, H. N., Moehler, T., Xiang, R., Jonczyk, A., Gillies, S. D., Cheresh, D. A., Reisfeld, R. A. (1999). Synergy between an antiangiogenic integrin αv antagonist and an antibody-cytokine fusion protein eradicates spontaneous tumor metastases. *Proc Natl Acad Sci U S A* **96**,1591-6.

Mao, Y. and Finnemann, S. C. (2012). Essential diurnal Rac1 activation during retinal phagocytosis requires αvβ5 integrin but not tyrosine kinases FAK or MerTK. *Mol Biol Cell* **23**, 1104-14.

Mazzoni, F., Mao, Y. and Finnemann, S. C. (2019). Advanced analysis of photoreceptor outer segment phagocytosis by RPE cells in culture. *Methods Mol Biol* **1834**, 95-108.

Muñoz, L. E., Franz, S., Pausch, F., Furnrohr, B., Sheriff, A., Vogt, B., Kern, P. M., Baum, W., Stach, C., von Laer, D. et al. (2007). The influence on the immunomodulatory effects of dying and dead cells of annexin V. *J Leukoc Biol* **81**, 6-14.

Nandrot, E. F., Anand, M., Almeida, D., Atabai, K., Sheppard, D. and Finnemann, S. C. (2007). Essential role for MFG-E8 as ligand for αvβ5 integrin in diurnal retinal phagocytosis. *Proc Natl Acad Sci U S A* **104**, 12005-10.

Nandrot, E. F., Kim, Y., Brodie, S. E., Huang, X., Sheppard, D. and Finnemann, S. C. (2004). Loss of synchronized retinal phagocytosis and age-related blindness in mice lacking αvβ5 integrin. *J Exp Med* **200**, 1539-45.

Nandrot, E. F., Silva, K. E., Scelfo, C. and Finnemann, S. C. (2012). Retinal pigment epithelial cells use a MerTK-dependent mechanism to limit the phagocytic particle binding activity of αvβ5 integrin. *Biol Cell* **104**, 326-41.

Oling, F., Santos, J. S., Govorukhina, N., Mazeres-Dubut, C., Bergsma-Schutter, W., Oostergetel, G., Keegstra, W., Lambert, O., Lewit-Bentley, A. and Brisson, A. (2000). Structure of membrane-bound annexin A5 trimers: a hybrid cryo-EM - X-ray crystallography study. *J Mol Biol* **304**, 561-73.

Parinot, C., Rieu, Q., Chatagnon, J., Finnemann, S. C. and Nandrot, E. F. (2014). Large-scale purification of porcine or bovine photoreceptor outer segments for phagocytosis assays on retinal pigment epithelial cells. *J Vis Exp*. **94**, doi: 10.3791/52100.

Pfaffle, M., Ruggiero, F., Hofmann, H., Fernandez, M. P., Selmin, O., Yamada, Y., Garrone, R. and von der Mark, K. (1988). Biosynthesis, secretion and extracellular localization of anchorin CII, a collagen-binding protein of the calpactin family. *EMBO J* **7**, 2335-42.

Robertson, E. J. (1987). Embryo derived stem cell lines. In *Teratocarcinomas and embryonic stem cells: a practical approach*, (ed. E. J. Robertson), pp. 71-112. Oxford, UK: IRL Press.

Rosenbaum, S., Kreft, S., Etich, J., Frie, C., Stermann, J., Grskovic, I., Frey, B., Mielenz, D., Poschl, E., Gaipl, U. et al. (2011). Identification of novel binding partners (annexins) for the cell death signal phosphatidylserine and definition of their recognition motif. *J Biol Chem* **286**, 5708-16.

Ruggiero, L., Connor, M. P., Chen, J., Langen, R. and Finnemann, S. C. (2012). Diurnal, localized exposure of phosphatidylserine by rod outer segment tips in wild-type but not Itgb5$^{-/-}$ or Mfge8$^{-/-}$ mouse retina. *Proc Natl Acad Sci U S A*. **109**, 8145-8.

Savill, J., Dransfield, I., Hogg, N. and Haslett, C. (1990). Vitronectin receptor-mediated phagocytosis of cells undergoing apoptosis. *Nature* **343**, 170-3.

Schlaepfer, D. D., Jones, J. and Haigler, H. T. (1992). Inhibition of protein kinase C by annexin V. *Biochemistry* **31**, 1886-91.

Segawa, K. and Nagata, S. (2015). An apoptotic 'eat me' aignal: Phosphatidylserine exposure. *Trends Cell Biol* **25**, 639-650.

Sethna, S. and Finnemann, S. C. (2013). Analysis of photoreceptor rod outer segment phagocytosis by RPE cells in situ. *Methods Mol Biol* **935**, 245-54.

Tzima, E., Trotter, P. J., Orchard, M. A. and Walker, J. H. (2000). Annexin V relocates to the platelet cytoskeleton upon activation and binds to a specific isoform of actin. *Eur J Biochem* **267**, 4720-30.

Wang, J., Liu, J., Cao, Y., Hu, M. and Hua, Z. (2017). Domain IV of annexin A5 is critical for binding calcium and guarantees its maximum binding to the phosphatidylserine membrane. *Molecules* 22, E2256.

West, K. A., Yan, L., Shadrach, K., Sun, J., Hasan, A., Miyagi, M., Crabb, J. S., Hollyfield, J. G., Marmorstein, A. D. and Crabb, J. W. (2003). Protein database, human retinal pigment epithelium. *Mol Cell Proteomics* **2**, 37-49.

Young, R. W. (1967). The renewal of photoreceptor cell outer segments. *J Cell Biol* **33**, 61-72.

Young, R. W. and Bok, D. (1969). Participation of the retinal pigment epithelium in the rod outer segment renewal process. *J Cell Biol* **42**, 392-403.

Figures

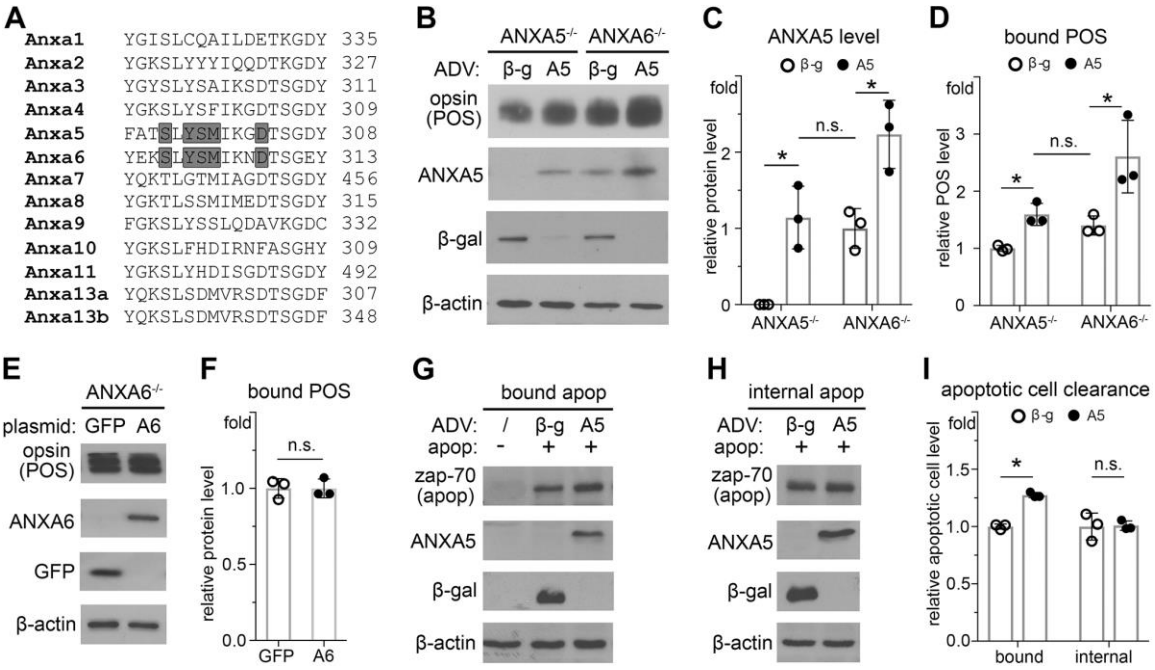

Figure 1. Annexin A5 promotes binding for phagocytic clearance of POS and apoptotic cells by MEFs. A. Alignment of the human annexin family. Gray boxes show integrin β5 binding domain of ANXA5. **B-I.** ANXA5$^{-/-}$ or ANXA6$^{-/-}$ MEFs as indicated were infected with recombinant adenoviruses encoding β-gal (β-g) or ANXA5 (A5) or transfected with plasmids encoding GFP or ANXA6 (A6) were challenged with POS or apoptotic cells at 20^{o}C for 1 h. Whole cell lysate representing equal numbers of cells were analyzed by immunoblotting with antibodies as indicated. **B.** Representative immunoblots showing bound POS-opsin and cellular proteins as indicated of MEFs infected as indicated. **C.** Comparison of ANXA5 protein levels relative to β-actin. ANXA5 content of ANXA6$^{-/-}$ MEFs expressing β-gal was set as 1. **D.** Quantification of POS binding by MEFs infected as indicated. Bars show bound POS relative to bound POS of ANXA5$^{-/-}$ MEFs expressing β-gal. **E.** Representative immunoblots showing bound POS-opsin of ANXAA6$^{-/-}$ MEFs transfected as indicated. **F.** Quantification of POS binding by ANXA6$^{-/-}$ MEFs. Bars show bound POS level relative to ANXA6$^{-/-}$ MEF expressing GFP. **G-H.** Representative immunoblots showing bound (**G**) and internalized (**H**) apoptotic cells (apop) by ANXA5$^{-/-}$ MEFs infected as indicated. **I.** Quantification of bound and internalized apoptotic cells by ANXA5$^{-/-}$ MEFs. Bars show bound POS relative to ANXA5$^{-/-}$ MEFs expressing β-gal. All bar graphs show mean ± s.d., n = 3 independent experiments; asterisks indicate significant differences and n.s. indicates

difference not significant (**C**, **D**, **I**: two-way ANOVA with Tukey's test; **F**: unpaired Student's two-tailed t-test).

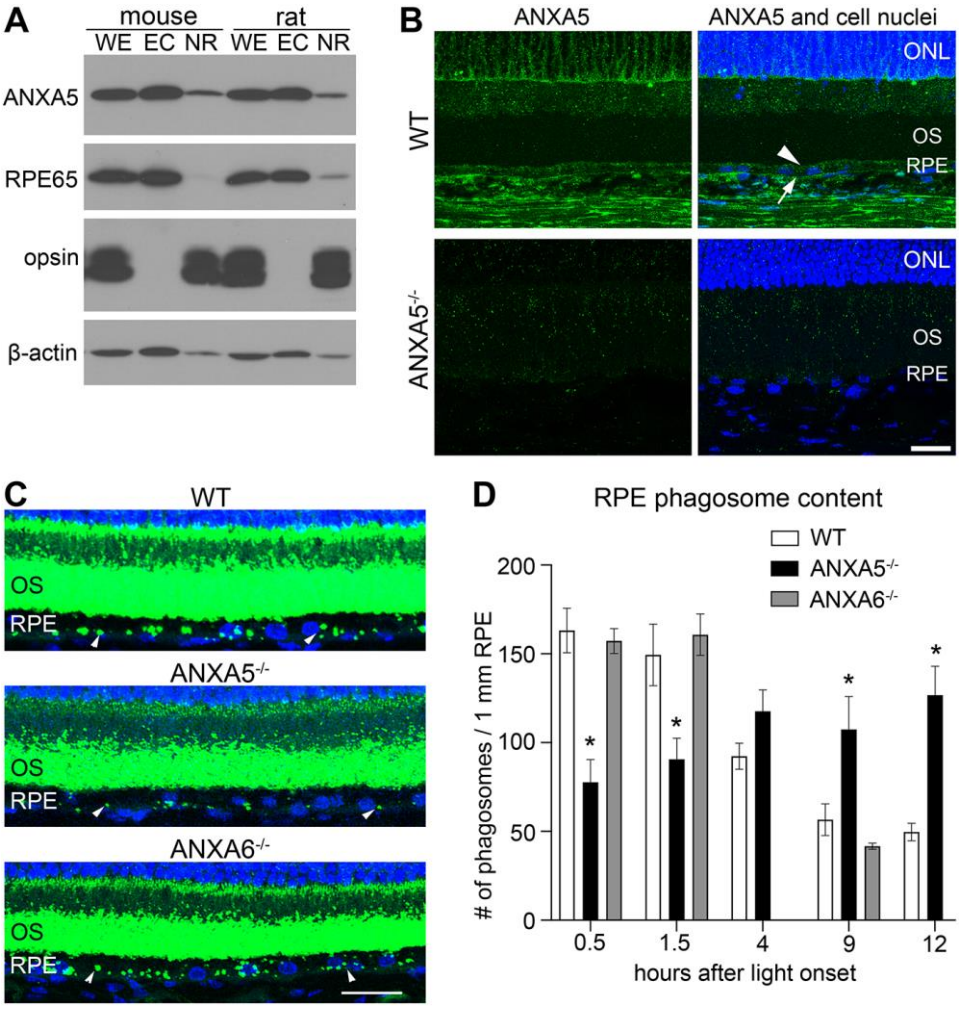

Figure 2. Deletion of ANXA5 but not ANXA6 abolishes the diurnal phagocytic rhythm of the RPE *in vivo*. A. Representative immunoblots showing ANXA5 and marker proteins as indicated in mouse and rat eye tissue lysates. W: whole eye without lens; E: posterior eyecup with RPE and choroid but without neural retina; R: neural retina. **B**. Representative images showing maximal projections of WT and ANXA5$^{-/-}$ mouse eye sections showing ANXA5 (green) and nuclei counterstain (blue). Arrows indicate ANXA5 at the interface of the apical, phagocytic surface of the RPE and photoreceptor outer segments (OS). ONL, outer nuclear layer. Scale bar: 20 µm. **C**. Representative images showing maximal projections of WT, ANXA5$^{-/-}$ and ANXA6$^{-/-}$ mouse eye sections showing opsin (green) and nuclei counterstain (blue). Mice were sacrificed 1.5 h after light onset. Example POS phagosomes in the RPE are indicated by arrowheads. Scale bar: 20 µm. **D.** Quantification of POS phagosomes in the RPE from experiments as in **C** from WT (white bars), ANXA5$^{-/-}$ (black bars) and ANXA6$^{-/-}$ (gray bars) mice sacrificed at select times after light onset as indicated.

Data are expressed as mean ± s.d.; eyes from 5 ANXA5$^{-/-}$ mice, 3 ANXA6$^{-/-}$ mice and 4 WT mice and 6 sections per eye were examined for each time point; asterisks indicate significant differences (two-way ANOVA with Tukey's test).

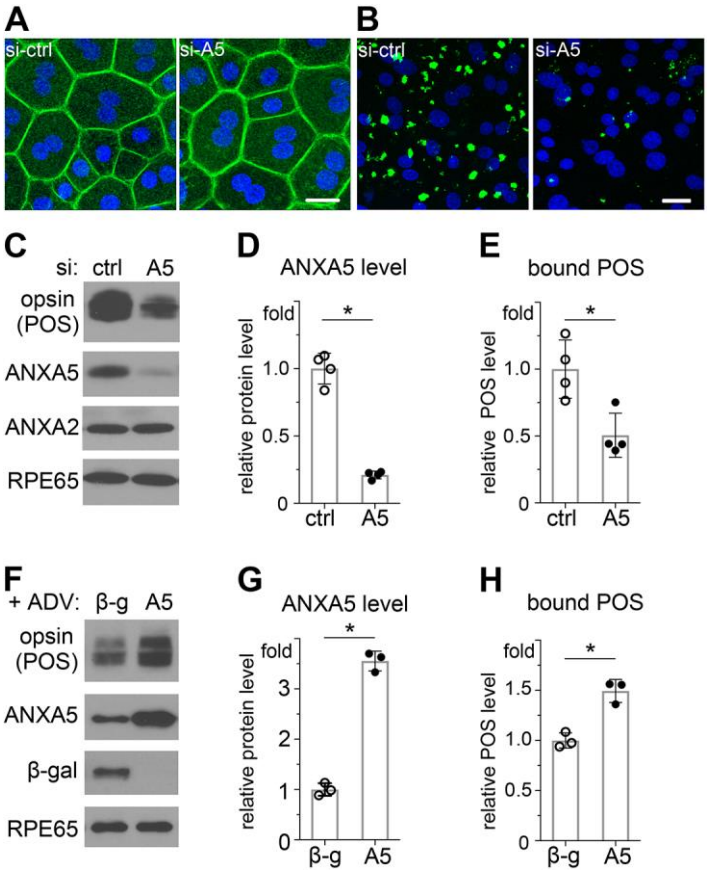

Figure 3. Silencing or overexpressing annexin A5 is sufficient to reduce or increase POS binding by RPE cells, respectively. **A**. Representative images of F-actin labeling (green) and cell nuclei (blue) showing normal morphology of primary rat RPE cells transfected with control siRNA (si-ctrl) or ANXA5-specific siRNA (si-A5). Scale bar: 20 μm. **B-H.** RPE cells were transfected with si-RNA as in **A** or infected with adenovirus to overexpress β-gal (β-g) or ANXA5 (A5) followed by POS challenge at 20°C for 1 h. **B.** Representative images show bound POS (green; nuclei in blue) of RPE cells transfected with siRNA as indicated. Scale bar: 20 μm. **C.** Representative immunoblots showing bound POS-opsin and cellular proteins as indicated in RPE cells transfected with siRNA as indicated. **D.** Comparison of ANXA5 protein levels normalized to RPE65, which served as loading control. ANXA5 level of RPE cells transfected with si-ctrl was set as 1. **E.** Quantification of POS binding by RPE cells transfected with siRNA as indicated. Level of bound POS by RPE cells transfected with si-ctrl was set as 1. **F.** Representative immunoblots showing bound POS-opsin of primary RPE cells overexpressing proteins as indicated. **G.** Comparison of ANXA5 protein levels normalized to RPE65, which served as

loading control. ANXA5 level of RPE cells expressing β-gal was set as 1. **H.** Quantification of POS binding by RPE cells overexpressing proteins as indicated. Level of bound POS by RPE cells expressing β-gal was set as 1. All bar graphs show mean ± s.d., n = 4 (**D, E**) or 3 (**G, H**) independent experiments; asterisks indicate significant differences (all, unpaired Student's two-tailed t-test).

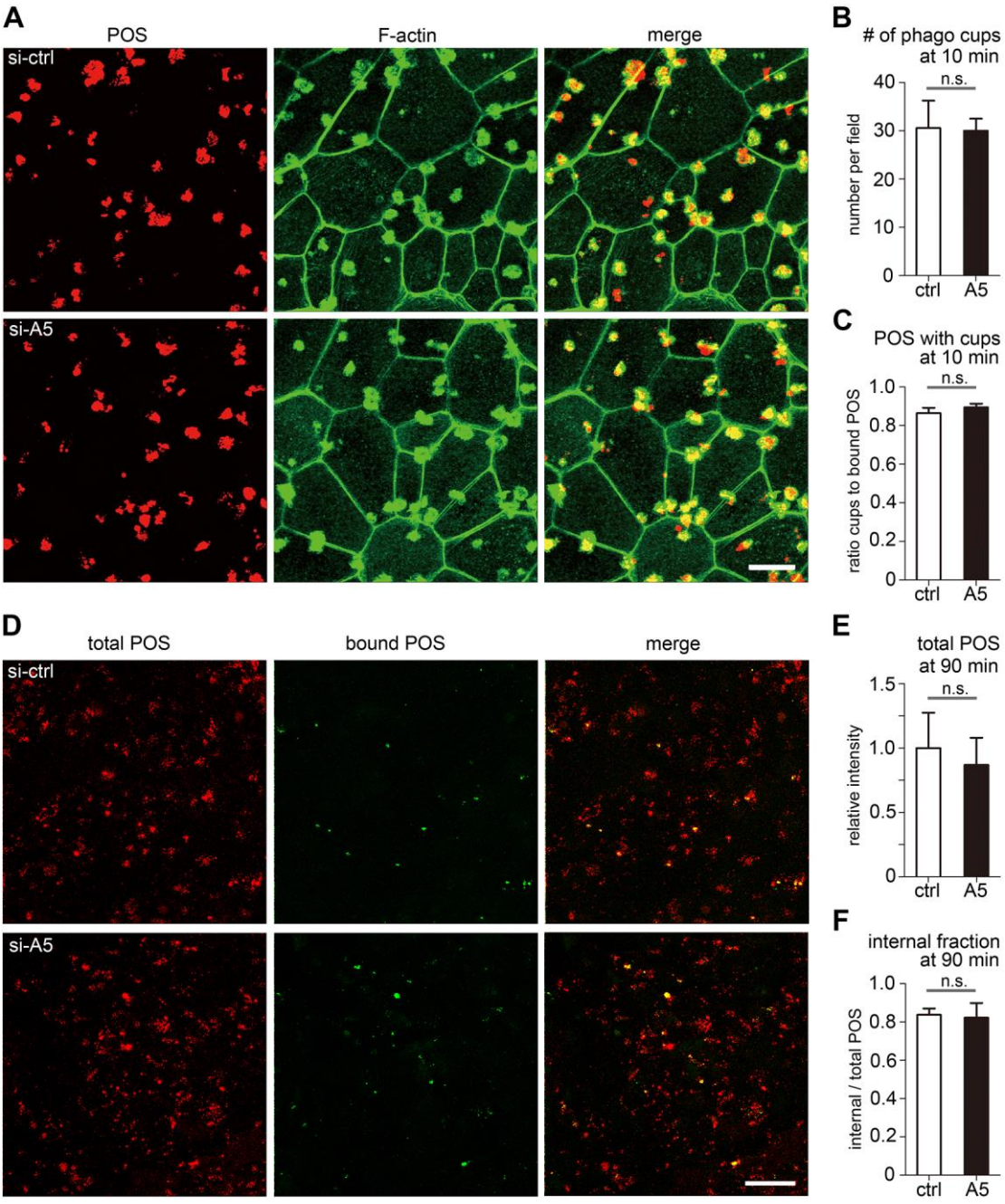

Figure 4. Annexin A5 does not contribute to POS phagocytic cup formation or internalization by RPE cells. Primary RPE cells transfected with si-ctrl or si-A5 as indicated were challenged with 5 POS per cell at 20°C for 1 h before wash, and continued incubation at 37°C for 10 min (**A-C**) or 90 min (**D-F**). **A.** Representative images after 10 min at 37°C of POS (red, left fields), F-actin (green, center fields) or merge (right) showing phagocytic cup formation of primary RPE cells. Scale bar: 20 μm. **B-C**. Quantification of the number of phagocytic cups per field and the ratio of phagocytic cups to total POS. **D**. Representative

images after 90 min at 37ºC of total POS (red, left fields), remaining bound POS (green, opsin surface labeling, center fields) and merge (right fields) showing most POS internalized. Scale bar: 50 µm. **E-F**. Quantification of total (bound plus internal) POS and fraction of internalized POS after 90 min at 37ºC by si-A5 transfected cells relative to values of control cells set as 1. All bar graphs show mean ± s.d.; n = 4 (**B, C**) or 5 (**E, F**) independent experiments and n.s. indicates difference not significant (all, unpaired Student's two-tailed t-test).

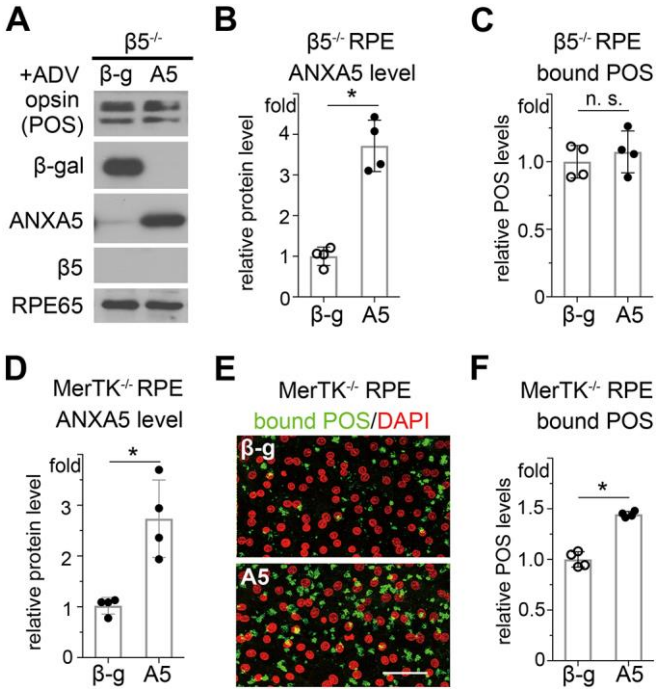

Figure 5. ANXA5 contributes to POS binding by RPE cells via αvβ5 integrin receptors and independently of MerTK receptors. $\beta5^{-/-}$ mouse and $MerTK^{-/-}$ RCS rat primary RPE cells infected with ADV-β-gal (β-g) or ADV-A5 (A5) were challenged with POS at 20ºC for 1 h. **A.** Representative immunoblots comparing bound POS-opsin and cellular protein levels as indicated of $\beta5^{-/-}$ RPE infected as indicated. **B, C.** Quantification of experiments as in **A** of ANXA5 protein levels (**B**) and bound POS (**C**), both normalized to RPE65, which served as loading control. Levels of ANXA5 and bound POS of RPE infected with ADV-β-gal were set as 1 for each parameter. **D.** Quantification of ANXA5 protein levels in $MerTK^{-/-}$RPE infected as indicated normalized to RPE65. ANXA5 level of $MerTK^{-/-}$ RPE infected with β-gal was set as 1. **E.** Representative images showing bound POS (green) and cell nuclei counterstain (red) of $MerTK^{-/-}$ RPE cells infected as indicated. Scale bar: 50 μm. **F.** Quantification of bound POS from images as in **E**. Bound POS of $MerTK^{-/-}$ RPE infected with β-gal were set as 1. All bar graphs show mean ± s.d.; n = 4 independent experiments; asterisks indicate significant differences and n.s. indicates difference not significant (all: unpaired Student's two-tailed t-test).

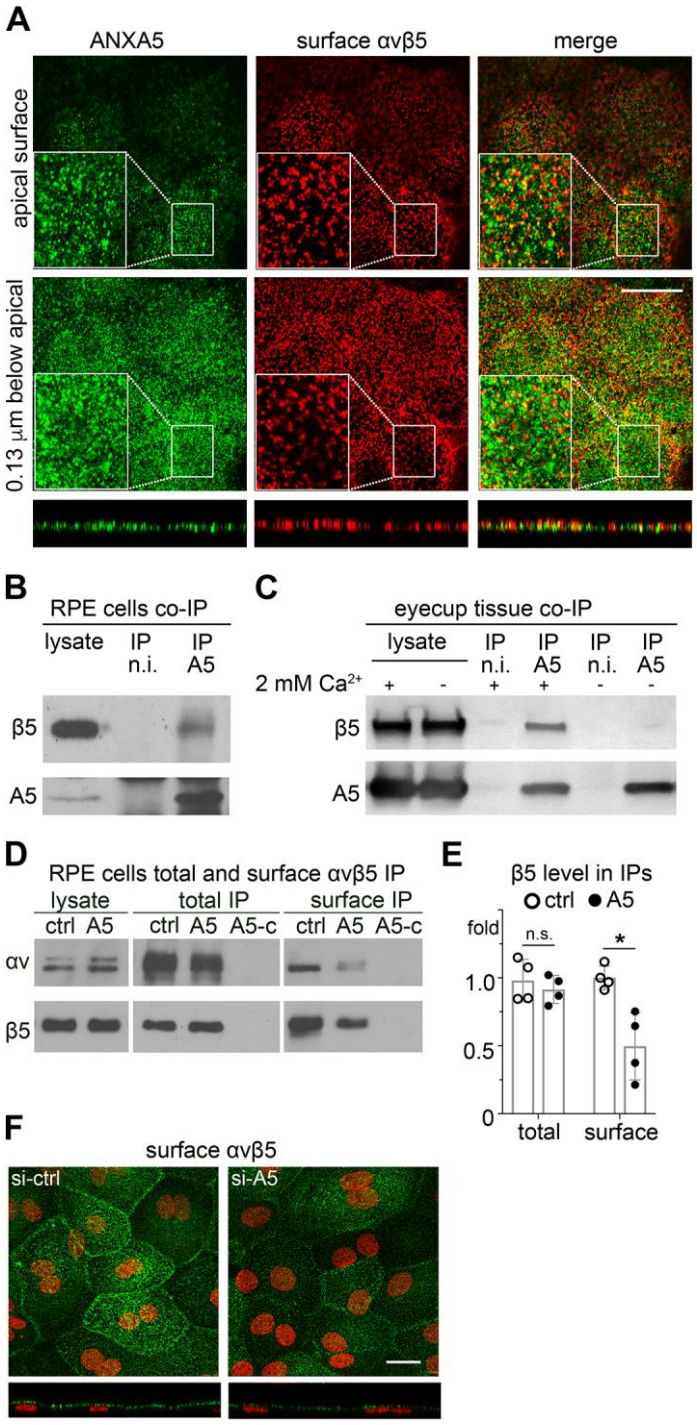

Figure 6. The functions of ANXA5 and αvβ5 integrin in particle binding are interdependent. β5$^{-/-}$ MEFs or ANXA5$^{-/-}$ MEFs were challenged with POS at 20°C for 1 h. Whole cell lysates representing equal numbers of cells were analyzed by immunoblotting with antibodies as indicated. **A.** Representative immunoblots showing bound POS-opsin and relevant markers of β5$^{-/-}$ MEFs and ANXA5$^{-/-}$ MEFs as indicated transfected with siRNA as indicated. ANXA5$^{-/-}$ MEFs were tested as control for ANXA5 siRNA specificity. **B.**

Quantification of ANXA5 levels from experiments as in **A**. Bars show ANXA5 relative to ANXA5 of $\beta5^{-/-}$ MEFs treated with si-ctrl, which was set as 1. **C.** Quantification of bound POS from experiments as in **A**. Bars of si-A5 show relative bound POS compared to the same MEFs treated with si-ctrl, whose bound POS were set as 1. **D.** Representative immunoblots showing bound POS and relevant markers in $\beta5^{-/-}$ MEFs infected with adenovirus to express β-gal or ANXA5 as indicated. **E.** Quantification of relative ANXA5 levels from experiments as in **D** with ANXA5 level of β-gal expressing cells set as 1. **F.** Quantification of relative bound POS from experiments as in **D** with bound POS of β-gal expressing cells set as 1. **G.** Representative immunoblots showing bound POS and relevant markers in $ANXA5^{-/-}$ MEFs infected with adenovirus to express GFP or β5-GFP as indicated. **H.** Quantification of relative β5 integrin levels from experiments as in **G** with levels of GFP expressing cells set as 1. **I.** Quantification of relative bound POS from experiments as in **G** with bound POS of GFP expressing cells set as 1. **J.** Representative images of $ANXA5^{-/-}$ MEFs infected to express GFP (left panel) or β5-GFP (right panel) with overlay shown of GFP fluorescence in green and αvβ5 receptor antibody surface labeling in red. Cells were live labeled on ice with αvβ5 receptor antibody and secondary antibody before fixation. Note that αvβ5 receptor antibody does not recognize endogenous mouse αvβ5 integrin. Scale bar: 10 μm. **K.** Representative immunoblot comparing the amount of bound POS-opsin, ANXA5, β5 integrin, and α-tubulin as loading control in WT, $ANXA5^{-/-}$ and $\beta5^{-/-}$ MEFs as indicated. Duplicate samples were tested. Samples were fed with POS in the presence of 1% water as control (ctrl) or in the presence of cilengitide αv integrin inhibitor (inh). **L.** Quantification of the amount of bound POS from samples as shown in **K**. Gray bars show POS binding of water control cells, white bars show binding in the presence of cilengitide of different MEFs as indicated. Relative values are shown compared to POS bound by control WT MEFs, which were set as 1. All bar graphs show mean ± s.d.; n = 3 (**B, C, E, F,** $\beta5^{-/-}$ MEFs in **L**) or 4 (**H, I,** WT and $ANXA5^{-/-}$ MEFs in **L**) independent experiments; asterisks indicate significant differences and n.s. indicates difference not significant (**B, C, L**: two-way ANOVA with Tukey's test; **E, F, H, I**: unpaired Student's two-tailed t-test).

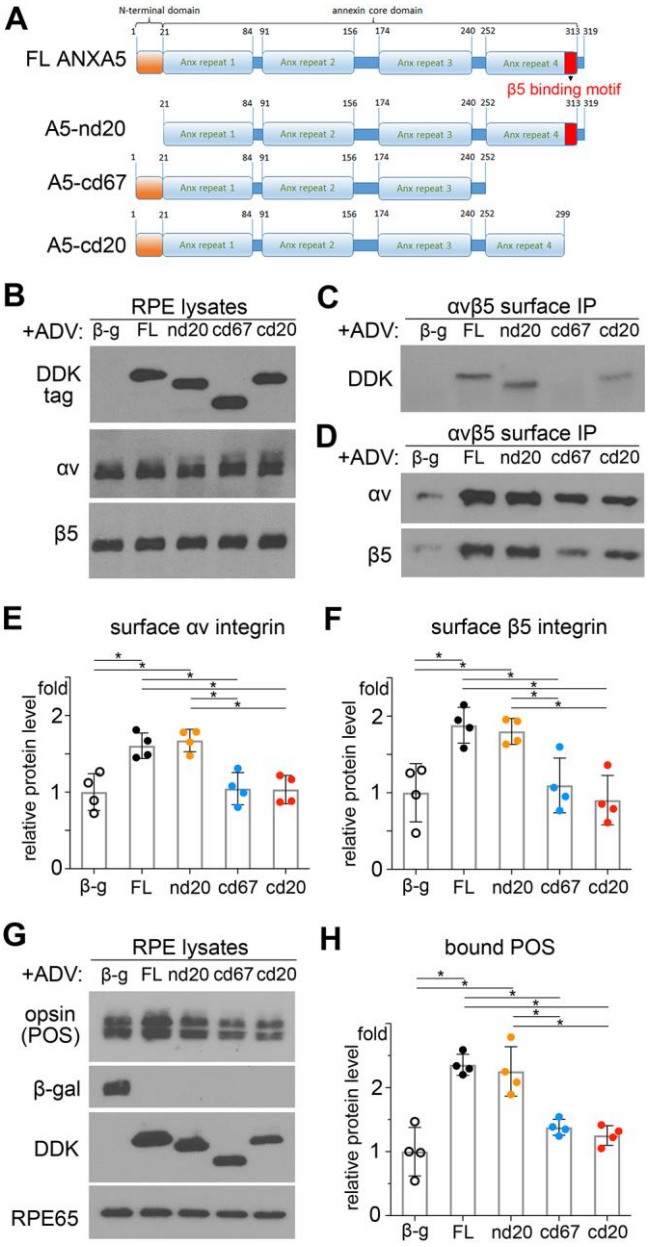

Figure 7. ANXA5 associates with αvβ5 and its silencing decreases specifically surface αvβ5 receptors in RPE cells. A. Live staining of αvβ5 surface receptors (red) followed by fixation, permeabilization and ANXA5 staining (green) in primary RPE cells. The representative field shows single confocal x-y scans of the apical surface and of the same field at a plane 0.13 µm below as indicated. Scale bar: 20 µm. X-z scans are also shown. **B, C.** IP of ANXA5 and co-IP of β5 integrin in lysates of unpassaged primary rat RPE cells and rat eyecup tissues, respectively. For experiments in **B**, buffers contained 2 mM Ca^{2+}, while buffers with and without Ca^{2+} were tested in **C**, as indicated. **D.** Representative immunoblots of lysate, total αvβ5 receptor IP, and surface αvβ5 receptor IP showing levels of αv and β5 integrin subunits in primary rat RPE cells transfected with si-ctrl or si-A5 as indicated. **E.**

Quantification of experiments as in **D**. Bars show relative β5 integrin levels with levels in cells transfected with si-ctrl set as 1. Graph shows mean ± s.d.; n = 4 independent experiments; an asterisks indicates significant difference and n.s. indicates difference not significant (both unpaired Student's two-tailed t-test). **F**. Representative images of surface αvβ5 receptor labeling in primary RPE cells treated with si-ctrl or si-A5 as indicated. Fields show merge of αvβ5 integrin (green) and nuclei (red) maximum projections. Scale bar: 20 µm.

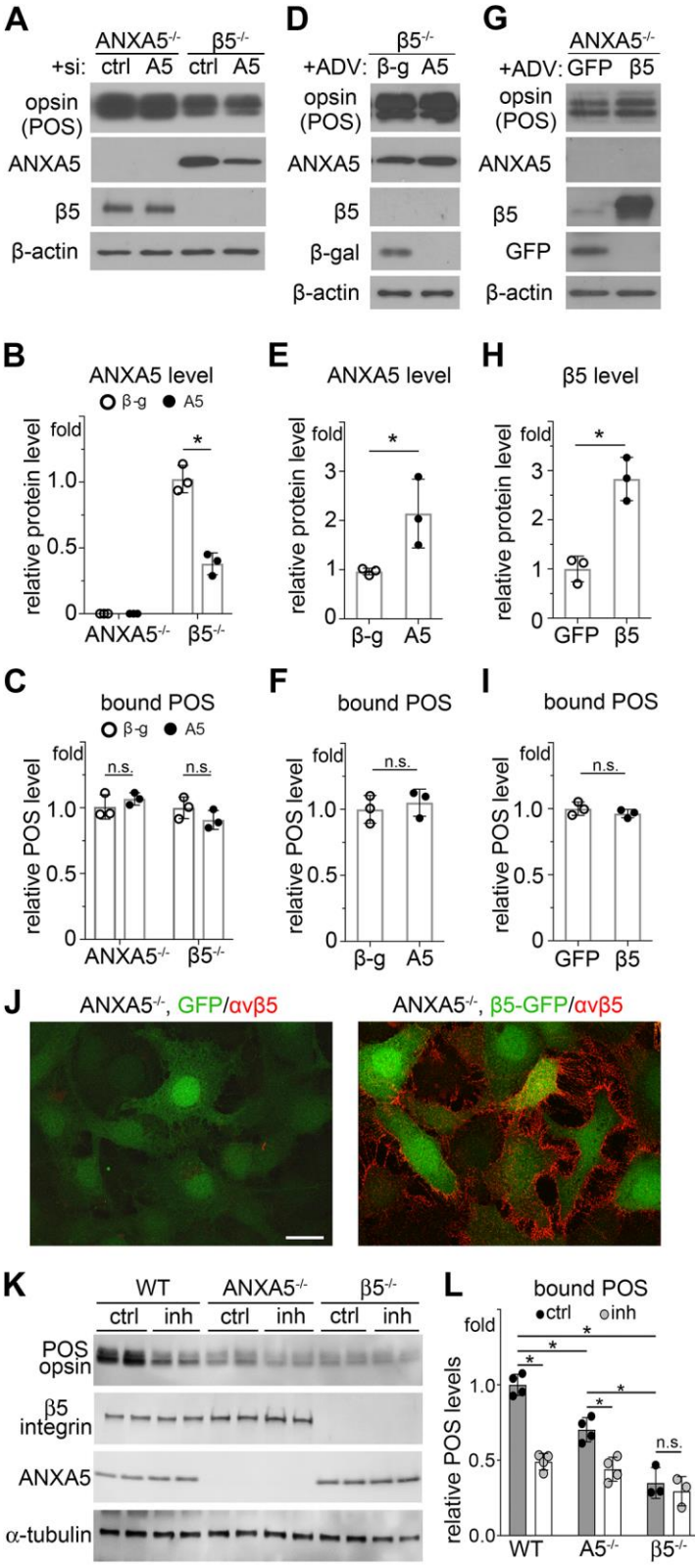

Figure 8. ANXA5 activity in regulating surface αvβ5 integrin and POS binding requires the β5 integrin binding motif in C-terminal annexin repeat 4 but not the ANXA5 unique N-terminus. A. Scheme of full length and truncated ANXA5 proteins studied. **B.**

Representative immunoblot comparing protein levels of ANXA5 variants, αv and β5 integrin subunits. **C.** Representative immunoblots of co-isolated ANXA5 variants from surface αvβ5 receptor IPs in rat primary RPE cells expressing ANXA5 variants tagged with DDK or β-gal as control. **D.** Representative immunoblots of surface IP of αvβ5 integrin complex comparing levels of integrin αv and β5 in RPE cells infected as indicated. **E-F.** Quantification of integrin αv (**E**) and β5 (**F**) from the surface IP samples shown in **D** and compared to levels of these proteins in RPE cells expressing β-gal, which was set as 1. **G.** Representative immunoblot comparing the amount of bound POS-opsin, ANXA5 variants tagged with DDK, β-gal and RPE65 as loading control in RPE cells infected as indicated. **H.** Quantification of the amount of bound POS from samples as shown in **G**. Relative values are shown compared to POS bound by RPE cells expressing β-gal, which were set as 1. All bars show mean ± s.d.; n = 4 independent experiments; asterisks indicate significant differences (all, one-way ANOVA with Tukey's test).

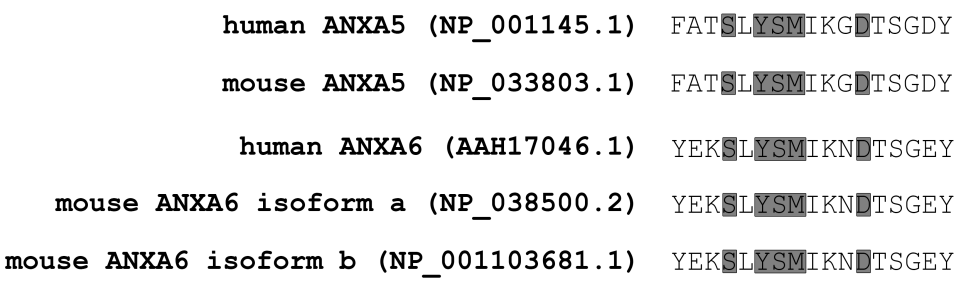

Figure S1. The integrin β5 binding motif in ANXA5 and ANXA6 is conserved between human and mouse. Gray boxes show the published integrin β5 binding motif of ANXA5.

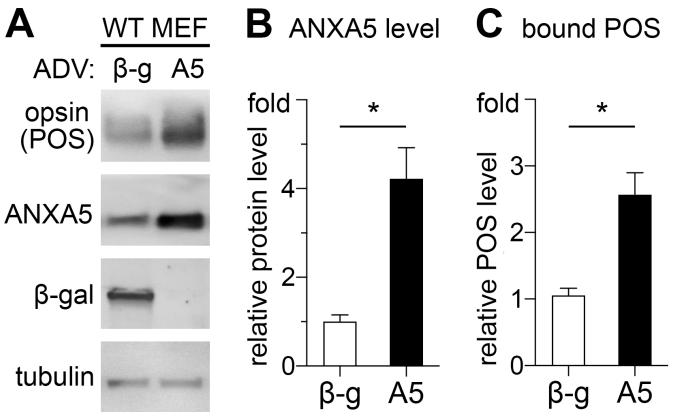

Figure S2. ANXA5 overexpression increases POS binding by WT MEFs. WT MEFs were infected with recombinant adenoviruses encoding β-gal (β-g) or ANXA5 (A5) before challenge with POS at 20°C for 1 h. Whole cell lysate representing equal numbers of cells were analyzed by immunoblotting with antibodies as indicated. **A.** A representative immunoblot shows bound POS-opsin and cellular proteins as indicated. A single blot membrane is shown probed sequentially to detect relevant proteins. **B.** Quantification of ANXA5 of WT MEFs using densitometry of immunoblots as shown in A. ANXA5 levels are normalized to ANXA5 of WT MEFs expressing β-gal, which is set as 1. **C.** Quantification of bound POS of WT MEFs using densitometry of immunoblots as shown in A. Bound POS are normalized to bound POS of WT MEFs expressing β-gal, which is set as 1. Data in B and C are expressed as mean ± s.d.; n = 6 independent experiments with duplicate samples each.

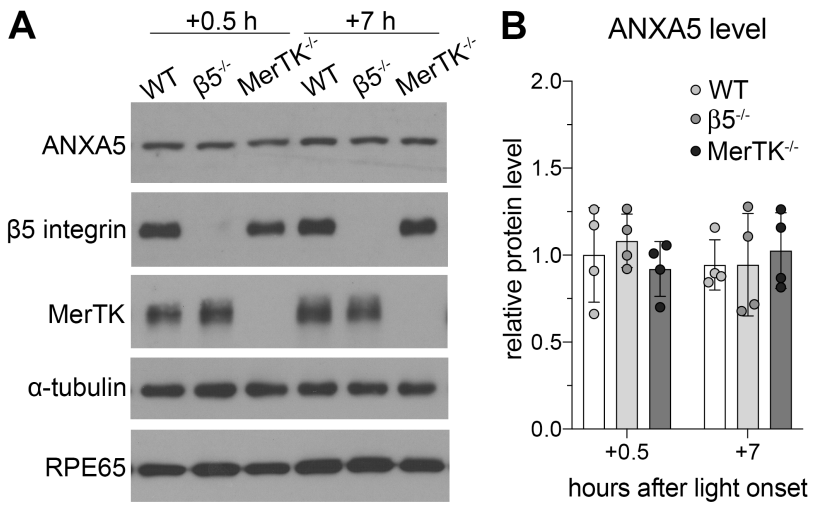

Figure S3. ANXA5 protein levels are the same in RPE/choroid tissues of WT, β5$^{-/-}$ and MerTK$^{-/-}$ mice. A. Representative immunoblots showing ANXA5 and marker proteins as indicated in RPE/choroid tissues from WT, β5$^{-/-}$ and MerTK$^{-/-}$ mice. Mice were sacrificed at 0.5 h or 7 h after light onset as indicated. **B.** Comparison of ANXA5 protein levels relative to the RPE specific marker RPE65. ANXA5 content of WT mice at 0.5 h after light onset was set as 1. Data are expressed as mean ± s.d.; eyes from 4 mice per time point per group.

Table S1. Primary antibodies used in this study. Abbreviations:

IB: immunoblotting; IF: immunofluorescence.

	Company	Catalog #	Dilution
rhodopsin (clone B630)	N/A	N/A	IB: 1:1000; IF: 1:100
annexin A5	Hyphen Biomed	PA120A	IB: 1:500; IF: 1:100
β-galactosidase	Abcam	ab4761	IB: 1:2000
annexin A2	BD Transduction	610068	IB: 1:10000
αv integrin	BD Transduction	611013	IB: 1:500
β-catenin	BD Transduction	610154	IF: 1:200
β-actin	Millipore-Sigma	M4758	IB: 1:2000
annexin A6	Santa Cruz	sc-1931	IB: 1:500
β5 integrin (H-96)	Santa Cruz	sc-14010	IB: 1:400
GFP	Santa Cruz	sc-9996	IB: 1:2000; IF: 1:100
αvβ5 integrin (clone P1F6)	BioLegend	MMS-474R	live IF: 1:50
RPE65	Genetex	GTX103472	IB: 1:3000
α-tubulin	Abcam	ab7291	IB: 1:3000
zap70	Cell Signaling	99F2	IB: 1:500

Table S2. Primers used to generate ANXA5 mutants.

ID	Sequence
A5-FL	forward: GCAGCGATCGCCATGGCTACGAGAGGCAC
	reverse: ATTACGCGTGTCATCCTCGCCCCCGCA
A5-nd20	forward: ATT GCGATCGCATG CTTCGGAAGGCCATGAAAG
	reverse: ATT ACGCGT GTCATCCTCGCCCCCGCA
A5-cd67	forward: GCAGCGATCGCCATGGCTACGAGAGGCAC
	reverse: GCAACGCGTGGTCTCTGCAAGGTAGGC
A5-cd20	forward: GCAGCGATCGCCATGGCTACGAGAGGCAC
	reverse: GCAACGCGTCTTGATCATAGAGTACAGGGAGGTGG

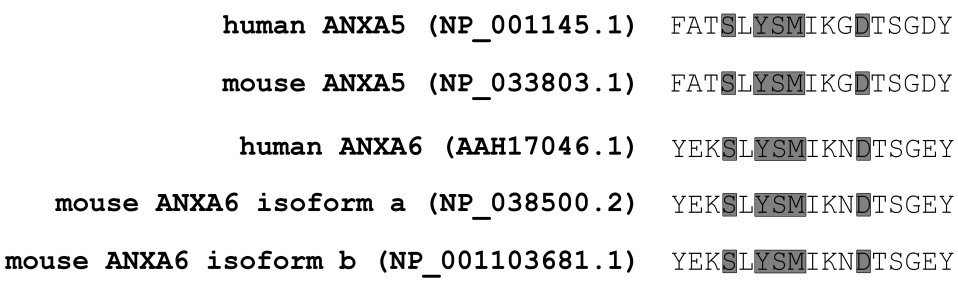

Figure S1. The integrin β5 binding motif in ANXA5 and ANXA6 is conserved between human and mouse. Gray boxes show the published integrin β5 binding motif of ANXA5.

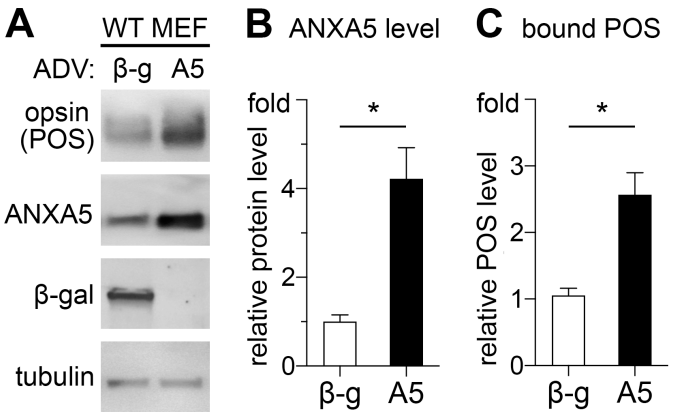

Figure S2. ANXA5 overexpression increases POS binding by WT MEFs. WT MEFs were infected with recombinant adenoviruses encoding β-gal (β-g) or ANXA5 (A5) before challenge with POS at 20°C for 1 h. Whole cell lysate representing equal numbers of cells were analyzed by immunoblotting with antibodies as indicated. **A.** A representative immunoblot shows bound POS-opsin and cellular proteins as indicated. A single blot membrane is shown probed sequentially to detect relevant proteins. **B.** Quantification of ANXA5 of WT MEFs using densitometry of immunoblots as shown in A. ANXA5 levels are normalized to ANXA5 of WT MEFs expressing β-gal, which is set as 1. **C.** Quantification of bound POS of WT MEFs using densitometry of immunoblots as shown in A. Bound POS are normalized to bound POS of WT MEFs expressing β-gal, which is set as 1. Data in B and C are expressed as mean ± s.d.; n = 6 independent experiments with duplicate samples each.

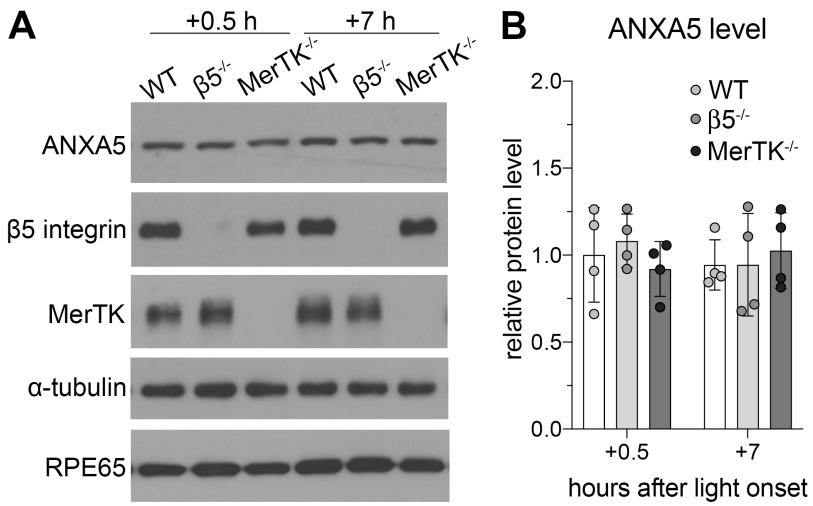

Figure S3. ANXA5 protein levels are the same in RPE/choroid tissues of WT, β5$^{-/-}$ and MerTK$^{-/-}$ mice. A. Representative immunoblots showing ANXA5 and marker proteins as indicated in RPE/choroid tissues from WT, β5$^{-/-}$ and MerTK$^{-/-}$ mice. Mice were sacrificed at 0.5 h or 7 h after light onset as indicated. **B.** Comparison of ANXA5 protein levels relative to the RPE specific marker RPE65. ANXA5 content of WT mice at 0.5 h after light onset was set as 1. Data are expressed as mean ± s.d.; eyes from 4 mice per time point per group.

Table S1. Primary antibodies used in this study. Abbreviations:

IB: immunoblotting; IF: immunofluorescence.

	Company	Catalog #	Dilution
rhodopsin (clone B630)	N/A	N/A	IB: 1:1000; IF: 1:100
annexin A5	Hyphen Biomed	PA120A	IB: 1:500; IF: 1:100
β-galactosidase	Abcam	ab4761	IB: 1:2000
annexin A2	BD Transduction	610068	IB: 1:10000
αv integrin	BD Transduction	611013	IB: 1:500
β-catenin	BD Transduction	610154	IF: 1:200
β-actin	Millipore-Sigma	M4758	IB: 1:2000
annexin A6	Santa Cruz	sc-1931	IB: 1:500
β5 integrin (H-96)	Santa Cruz	sc-14010	IB: 1:400
GFP	Santa Cruz	sc-9996	IB: 1:2000; IF: 1:100
αvβ5 integrin (clone P1F6)	BioLegend	MMS-474R	live IF: 1:50
RPE65	Genetex	GTX103472	IB: 1:3000
α-tubulin	Abcam	ab7291	IB: 1:3000
zap70	Cell Signaling	99F2	IB: 1:500

Table S2. Primers used to generate ANXA5 mutants.

ID	Sequence
A5-FL	forward: GCAGCGATCGCCATGGCTACGAGAGGCAC
	reverse: ATTACGCGTGTCATCCTCGCCCCCGCA
A5-nd20	forward: ATT GCGATCGCATG CTTCGGAAGGCCATGAAAG
	reverse: ATT ACGCGT GTCATCCTCGCCCCCGCA
A5-cd67	forward: GCAGCGATCGCCATGGCTACGAGAGGCAC
	reverse: GCAACGCGTGGTCTCTGCAAGGTAGGC
A5-cd20	forward: GCAGCGATCGCCATGGCTACGAGAGGCAC
	reverse: GCAACGCGTCTTGATCATAGAGTACAGGGAGGTGG